Experiment on MHD Generator with a Large-Scale Superconducting Magnet (ETL Mark V)

S. Ikeda,* T. Masuda, * Y. Kusaka,†
T. Honda,† and Y. Aiyama‡
Electrotechnical Lab., Tokyo, Japan

EXPERIMENTAL and theoretical investigations were made of the Al_2O_3 coated peg-wall-type generator with a large-scale superconducting magnet. In Japan's MHD National Project, the many component apparatuses required for the MHD plant had been developed individually and these apparatuses had been combined into ETL Mark V and VI MHD generators in 1971. The ETL Mark V generator had as main components, a superconducting magnet, the cold-wall Faraday-type generating channel, and a combustor of 25-MW thermal input for the purpose of investigating the generating characteristics in a strong magnetic field. The details of the ETL Mark V generator were reported elsewhere.[1-6] Since the construction of this equipment, 27 thermal and three generating experiments have been carried out and the summary of these operations resulted in about 55 hours of thermal and about five hours of generating experiments. The maximum output power of 86 kW was generated in the first one, 193 kW in the second one, and 482 kW in the last one.

This note describes the results of the last generating experiment and experimental conditions are summarized in Table 1. The calculated gas temperatures were 3050K at the combustor and 2680K at the inlet of the generating section for the mass flow rate of 3 kg/sec. Though the combustion conditions were different, the measured gas temperature was 2860K at the inlet of the generating section on the other thermal experiment of 3 kg/sec. The power generating time was 3.3 hrs. The central magnetic field strength was 4.2 T. The generating channel had 50 pairs of electrodes which were made of sintered copper (30%)-tungsten (70%) as cathode and stainless steel (AISI 304) as anode. The estimated surface temperatures of cathode and anode were 600K and 900K, respectively. The electrode surface area was 18×100 mm^2 and electrode pitch was 36 mm. The cross-sectional area of the generating section was 150×100 mm^2 at inlet and 241×100 mm^2 at outlet and the length was 1764 mm. The generating characteristics were measured at each step of mass flow rate.

The generating channel was constructed with 50 pairs of side and electrode wall modules whose flow direction length was 108 mm.[1,2] The heat losses were calculated from measuring the water flow rate and temperature difference of every wall module. The heat loss and the fraction of the thermal input at the mass flow rate of 3 kg/sec were as follows: combustor – 2.26 MW, 9.1%, nozzle – 3.78 MW, 15.2%, total up to the inlet of the generating section – 6.04 MW, 24.3%; generating section – 1.93 MW, 7.8%; downstream up to the diffuser – 2.32 MW, 9.3%.

Figure 1 shows the heat flux distribution for the mass flow rates of 2 kg/sec and 3 kg/sec and the calculated value for 3 kg/sec. The position of the nozzle throat was $x = 0.7$ m; the inlet of the generating section was 0.91 m and the outlet was 2.67 m. The heat flux varied considerably in the case of short and open circuits and the averaged difference was 10-20% in the generating section. The maximum heat flux was 370 W/cm^2 at the vicinity of the nozzle throat at the mass flow rate of 3 kg/sec. The calculated value was different from the measured one and it was underestimated. In the quasi-one-dimensional calculation considering the effect of the boundary layer, the expression of the forced convective heat transfer was adopted, considering the effect of the wall roughness and Prandtl number. The surface wall temperature used in the calculation seems to be higher than the true value.

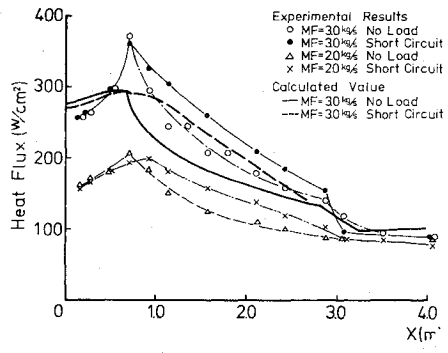

Fig. 1 Comparison of theoretical and experimental heat flux distributions.

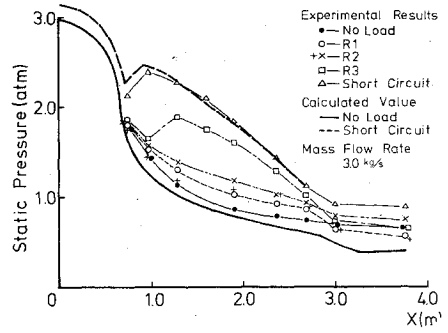

Fig. 2 Comparison of theoretical and experimental static pressure distributions.

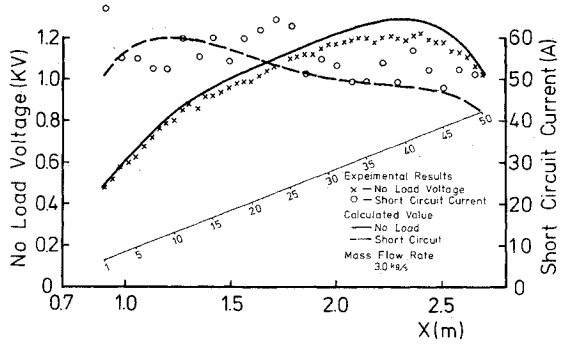

Fig. 3 Comparison of theoretical and experimental open voltage and short-circuit current distributions.

Figure 2 shows the static pressure distribution at each load for the mass flow rate of 3 kg/sec. The combustor pressures at no-load and short circuit were 3.39 and 3.52 atm, respectively. The flow was supersonic at the open circuit and subsonic at the short circuit. When the load was medium (R3), the shock wave occurred at the distance of $x = 1.1$ m. The calculated flow velocity (and Mach number) was 1190 m/sec (1.28) at the inlet and 1610 m/sec (1.8) at the outlet of the generating section in the case of the open circuit and 700 m/sec (0.72) and 860 m/sec (0.93) for short-circuit conditions. The analysis gives good agreement, but, when the shock wave occurs, the

Received June 11, 1976; revision received Aug. 13, 1976. The calculations were carried out using the code developed by K. Takano.

Index categories: Plasma Dynamics and MHD; Electric Power Generation Research.

*Senior Research Scientist, Energy Conversion Sect.

†Research Scientist, Energy Conversion Sect.

‡Chief of Extreme Technology Div.

Table 1 Experimental conditions

Flow rate, kg/sec					
Total	1.26	1.51	2.0	2.52	3.0
Diesel oil (C/H/S = 85.4/14.2/0.3)	0.2	0.257	0.37	0.482	0.592
Oxygen	0.682	0.87	1.245	1.62	1.985
KOH solution	0.036	0.044	0.059	0.074	0.089
Atomizing N_2	0.341	0.341	0.341	0.341	0.341
Thermal input, MW	8.4	10.8	15.6	20.3	24.9
Combustor pressure, atm	1.46	1.72	2.28	2.84	3.52
Running time, minutes	15	35	30	26	59

calculated pressure distribution shows considerable disagreement in the neighboring region. The position of the shock wave moves upstream as the load increases.

Figure 3 shows the open voltage and short-circuit current distribution for the mass flow rate of 3.0 kg/sec. The small numbers (1-50) in the figure indicate electrode numbers and their positions. The analysis gives extremely good agreement on open voltage. The small deviation is due to the leakage current, judging from the measurement by probes of the potential distribution in the Faraday direction. The decline of the voltage at the end of generating section is due to the steep drop of the magnetic field. The measured electrode drop by probe was about 400 V at the No. 14 electrode and about 500 V at the No. 26 electrode. The relatively large current could be extracted in spite of the large voltage drop of the cold boundary layer. The calculated short-circuit current shows some deviation from the measured value, especially in the downstream region.

The maximum output power of 482 kW and the total short-circuit current of 2820 A were obtained for the mass flow rate of 3 kg/sec. The Hall voltage (and Hall field intensity) for the mass flow rate of 3 kg/sec were 2525 V (19.61 V/cm), 2075 V (11.11 V/cm), 1685 V (7.84 V/cm), and 1160 V (5.88 V/cm) as load increased. The calculated maximum output power, total short-circuit current, and Hall voltage at short circuit were 429 kW, 2600 A, and 4000 V, respectively.

Concerning the superconducting magnet, a very long time is needed to cool and magnetize the magnet which was composed of the Nb-Ti-Zr coil of 13 tons and the support of 35 tons. The required time to cool the magnet from 300 K to 150 K by cold He gas was 124 hr, from 150 K to 50 K, by refrigerating operations was 97 hr, and from 50 K to 15 K was 25 hr. The time to liquify the He gas and charge the liquid He in a cryostat was 76 hr. The raising time (5-15 A/min) of the magnetic field until 4.2 T was 13 hr.

We may conclude that this generator can extract high output power and endure for a long time judging from the good durability at least for 12 hr, (4 hr × 3 times) under the thermal flux of 270 W/cm^2 at the nozzle throat for the mass flow rate of 2.5 kg/sec without any replenishment, and also based on the ETL Mark III's result of 230 hr endurance.

The quasi-one-dimensional analysis could predict the generating characteristics within an error of 15%. However, further work is needed to improve the understanding of the heat loss, the leakage current, and the electrode phenomena in regard to the seed compound.

References

[1]Fushimi, K., et al., "Construction of an MHD Generator with A Large-Scale Superconducting Magnet (ETL Mark V)", *Proceedings of the 13th Symposium on Engineering Aspects of MHD,* 1973, Stanford University, Stanford, Calif.

[2]Fushimi, K., et al., "Experiment on MHD Generator with a Large-Scale Superconducting Magnet", *Proceedings of the 14th Symposium on Engineering Aspects of MHD,* 1974, University of Tennessee Space Institute, Tullahoma, Tenn.

[3]Aiyama, Y., "Research on Superconducting Magnet System for MHD Project in Japan", *Proceedings of the 5th International Cryogenic Engineering Conference,* 1974, Kyoto, Japan.

[4]Aiyama, et al., "A Large Superconducting MHD Magnet", *Proceedings of the 5th International Cryogenic Engineering Conference,* 1974, Kyoto, Japan.

[5]Aiyama, Y., et al., "Helium Refrigerator-Liquifier System for MHD Generator", *Proceedings of the 5th International Cryogenic Engineering Conference,* 1974, Kyoto, Japan.

[6]Ikeda, S., et al., "Experiment on MHD Generator with a Large-Scale Superconducting Magnet", *Proceedings of the 15th Symposium on Engineering Aspects of MHD,* 1976, University of Pennsylvania, Philadelphia, Pa.

Skin Friction on a Flat Perforated Acoustic Liner

Donald R. Boldman* and Paul F. Brinich†
NASA Lewis Research Center, Cleveland, Ohio

Nomenclature

a = local speed of sound
b = cavity depth
C_f = skin friction coefficient
d = diameter of holes in perforated plate
f = frequency
L = reference length along acoustic liner
l = effective thickness of perforated plate (includes orifice end correction)
Re = Reynolds number
S = Strouhal number
U_∞ = freestream velocity
x = axial distance along wind tunnel wall
y = distance from wall
δ^* = boundary-layer displacement thickness
θ = boundary-layer momentum thickness
σ = ratio of hole area to total area on perforated plate
χ = linear reactance
$()_0$ = denotes condition at upstream station referenced to the virtual origin of the boundary layer

Introduction

IT has been well-established that acoustic treatment of the ducts in turbomachinery provides an effective means for reducing external noise levels. One type of acoustic material consists of an array of honeycomb cavities covered with a perforated plate with flow passing along it. However, the roughness associated with a perforated surface can increase the skin friction coefficient. Although much is known about roughness effects on friction for surfaces containing certain types of roughness elements such as sand grains, ribs, threads,

Received Aug. 4, 1976.
Index categories: Boundary Layers and Convective Heat Transfer – Turbulent; Aircraft Noise, Powerplant.

*Aerospace engineer, Fluid Physics and Chemistry Branch of the Physical Sciences Division. Member AIAA.